coatings

MDPI

Supplementary Materials: Dual Strategy Based on Quantum Dot Doping and Phenylethylamine Iodide Surface Modification for High-Performance and Stable Perovskite Solar Cells

Shulan Zhang [1], Renjie Chen [1], Mujing Qu [1], Biyu Long [1], Nannan He [1], Sumei Huang [1,2], Xiaohong Chen [1,2,*], Huili Li [1,2,3,*] and Tongtong Xuan [4,*]

[1] Engineering Research Center for Nanophotonics & Advanced Instrument, Ministry of Education, School of Physics and Electronic Science, East China Normal University, Shanghai 200241, China; shulann@163.com (S.Z.); 52184700021@stu.ecnu.edu.cn (R.C.); mjing2021@163.com (M.Q.); 17742615350@163.com (B.L.); shihnna@163.com (N.H.); smhuang@phy.ecnu.edu.cn (S.H.)

[2] Joint Institute of Advanced Science and Technology, East China Normal University, Shanghai 200241, China

[3] Chongqing Key Laboratory of Precision Optics, Chongqing Institute of East China Normal University, Chongqing 401120, China

[4] Fujian Key Laboratory of Surface and Interface Engineering for High Performance Materials, College of Materials, Xiamen University, Xiamen 361005, China

* Correspondence: xhchen@phy.ecnu.edu.cn (X.C.); hlli@phy.ecnu.edu.cn (H.L.); ttxuan@xmu.edu.cn (T.X.)

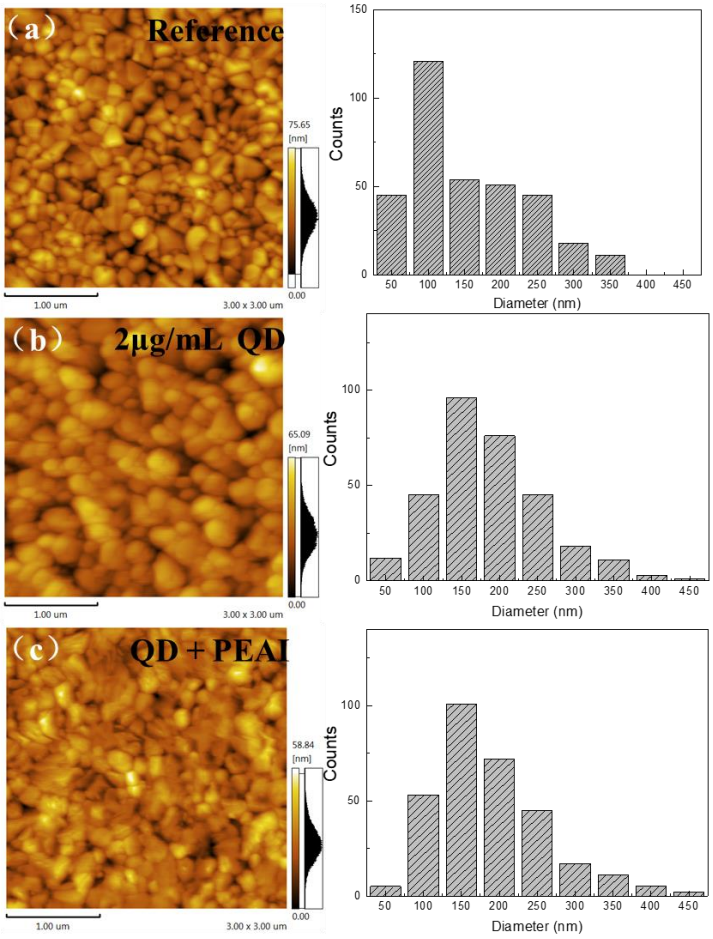

Figure S1. AFM images and grain size statistics of perovskite films modified with different conditions: (a) reference, (b) doped with 2 μg/mL $CsPbBr_3$ QDs, (c) jointly modified with 2 μg/mL $CsPbBr_3$ QDs and 2 mg/mL PEAI.

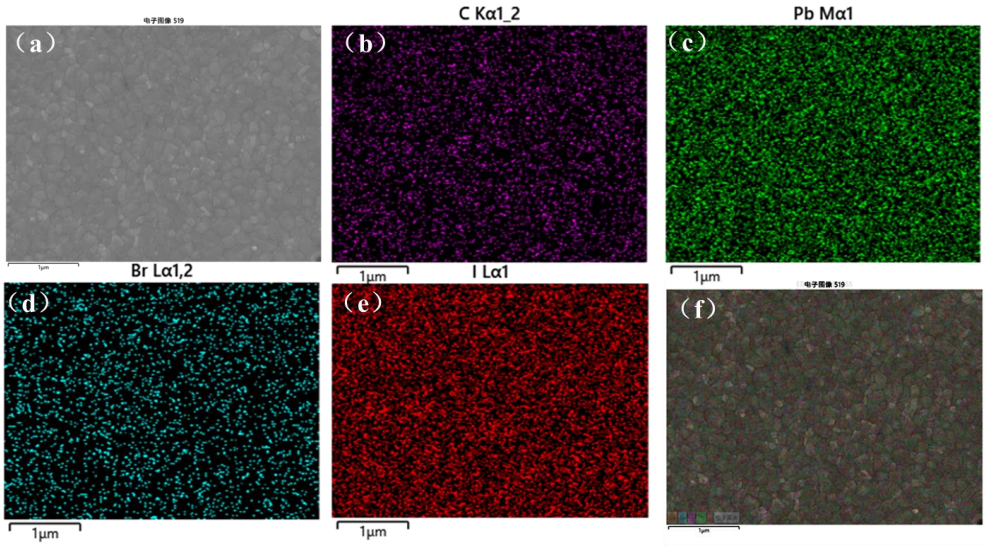

Figure S2. EDS mappings of PFs jointly modified with $CsPbBr_3$ QDs and PEAI: (a) SEM pattern, (b) C element, (c) Pb element, (d) Br element, (e) I element, (f) the combination of SEM and mappings.

Table S1 The parameters of (110) diffraction peak of PFs modified at different conditions.

Samples	Peak location (°)	Intensity (a.u.)	FWHM (°)
reference	13.97	1506	0.193
0.2 μg/mL QDs	13.99	1713	0.185
2 μg/mL QDs	14.01	2398	0.178
10 μg/mL QDs	14.04	1968	0.183
QDs+PEAI	14.01	2396	0.178

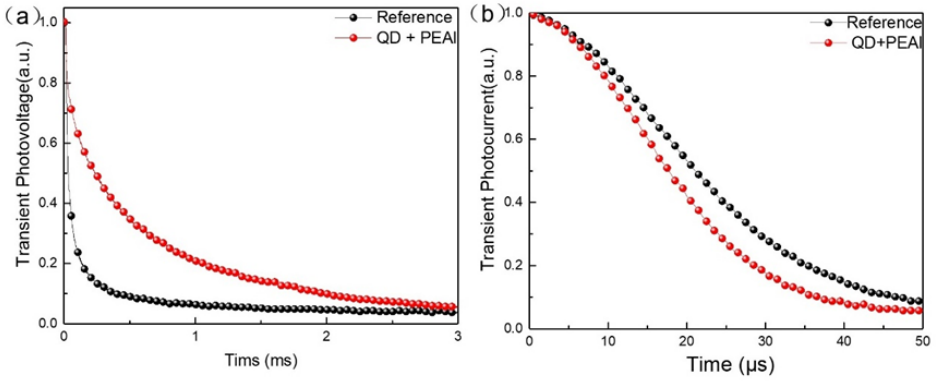

Figure S3. TPV (a) and TPC (b) decay curves of original and jointly-modified PSCs.

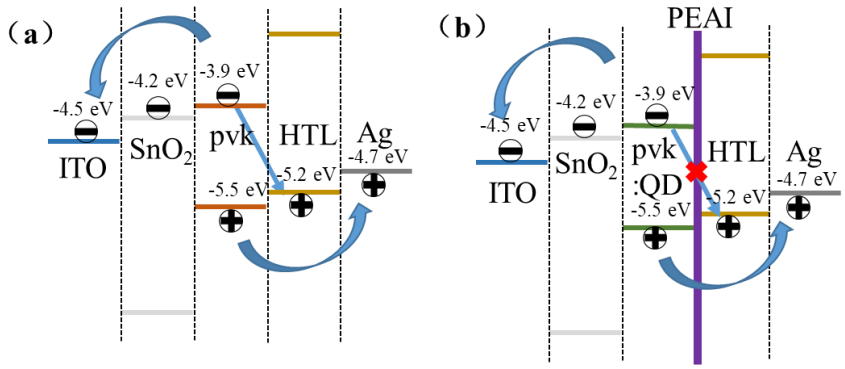

Figure S4. The energy alignment of reference and $CsPbBr_3$ QDs + PEAI modified PSCs.

The quantum tunneling effect is described as follows:

$$T = (C / A)^2 = Exp\left[-2\,d\sqrt{\frac{2m_n(qV_0-E)}{\hbar^2}}\right] \quad \text{(S-1)}$$

where T represents the transmission coefficient, C represents the transmission wave function, A represents the incident wave function, m_n represents the effective mass of the electron, ħ represents the reduced Planck constant, qV_0 represents the barrier height, and d represents the thickness of the tunneling layer.

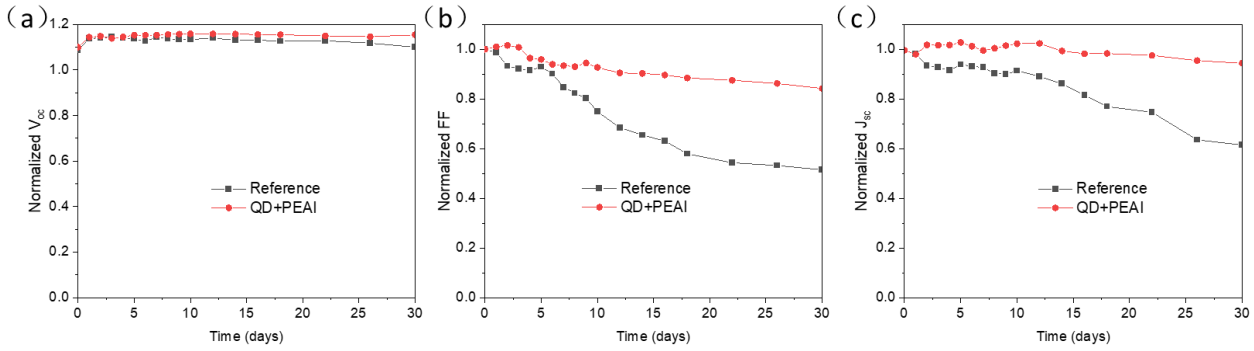

Figure S5. Aging curves of normalized V_{OC} (a)、FF(b) and J_{SC} (c) in air condition with a RH of 40% and RT (unpacked).

Table S2 Simple comparison of PCE MAPbI3 perovskite solar cells.

Perovskite	PCE_{max} (%)	Reference
$MAPbI_3$	19.11	[1]
$MAPbI_3$	20.06	[2]
$MAPbI_3$	20.22	[3]
$MAPbI_3$	20.23	[4]
$MAPbI_3$	20.46	[5]
$MAPbI_3$	20.46	[6]
$MAPbI_3$	20.46	[7]
$MAPbI_3$	20.93	[8]
$MAPbI_3$	21.04	This Work

References

1. Liu, R.; Wang, J.; Mak, C.H.; Du, M.; Li, F.-F.; Shen, H.-H.; Santoso, S.P.; Yu, E.T.; Yu, X.; Chu, P.K.; et al. Optimizing Black Phosphorus/Halide Perovskite Compositions by Scanning Photoelectrochemical Microscopy. *J. Electrochem. Soc.* **2022**, *169*, 096510, doi:10.1149/1945-7111/ac8d34.

2. Feng, Z.; Weng, C.; Hua, Y.; Chen, X.; Huang, S. Efficient and Stable Perovskite Solar Cells: The Effect of Octadecyl Ammonium Compound Side-Chain. *Chem. Eng. J.* **2023**, *475*, 146498, doi:10.1016/j.cej.2023.146498.

3. Lu, R.; Liu, Y.; Zhang, J.; Zhao, D.; Guo, X.; Li, C. Highly Efficient (200) Oriented MAPbI3 Perovskite Solar Cells. *Chem. Eng. J.* **2022**, *433*, 133845, doi:10.1016/j.cej.2021.133845.

4. Phase Control of Organometal Halide Perovskites for Development of Highly Efficient Solar Cells | ACS Applied Materials & Interfaces Available online: https://pubs.acs.org/doi/10.1021/acsami.2c22769 (accessed on 24 March 2024).

5. Yao, Y.; Hang, P.; Wang, P.; Xu, L.; Cui, C.; Xie, J.; Xiao, K.; Li, G.; Lin, P.; Liu, S.; et al. CsPbBr 3 Quantum Dots Assisted Crystallization of Solution-Processed Perovskite Films with Preferential Orientation for High Performance Perovskite Solar Cells. *Nanotechnology* **2020**, *31*, 085401, doi:10.1088/1361-6528/ab55a1.

6. Azadipyrromethene Dye-Assisted Defect Passivation for Efficient and Stable Perovskite Solar Cells | ACS Applied Materials & Interfaces Available online: https://pubs.acs.org/doi/full/10.1021/acsami.1c20923 (accessed on 24 March 2024).

7. Nguyen, M.H.; Kim, K.-S. Controlling the Grain Formation Process with Oleylamine and 4-Dimethylaminopyridine Additives for Efficient and Stable MAPbI3 Solar Cells. *Mater. Today Chem.* **2023**, *34*, 101799, doi:10.1016/j.mtchem.2023.101799.

8. Reinforcing the Efficiency and Stability of Perovskite Solar Cells Using a Cesium Sulfate Additive | Journal of Materials Science: Materials in Electronics Available online: https://link.springer.com/article/10.1007/s10854-023-10008-6 (accessed on 24 March 2024).